The postnatal injection of AAV9-FOXG1 rescues corpus callosum agenesis and other brain deficits in the mouse model of FOXG1 syndrome

Shin Jeon,[1,2,5] Jaein Park,[1,5] Shibi Likhite,[3,5] Ji Hwan Moon,[1,4] Dongjun Shin,[1] Liwen Li,[1] Kathrin C. Meyer,[3] Jae W. Lee,[1] and Soo-Kyung Lee[1]

[1]Department of Biological Sciences, College of Arts and Sciences, FOXG1 Research Center, University at Buffalo, The State University of New York (SUNY), Buffalo, NY 14260, USA; [2]Department of Systems Pharmacology & Translational Therapeutics, Institute for Immunology, University of Pennsylvania, Philadelphia, PA 19104, USA; [3]The Research Institute at Nationwide Children's Hospital, Columbus, OH 43205, USA; [4]Samsung Genome Institute, Samsung Medical Center, Seoul 06351, Korea

Heterozygous mutations in the *FOXG1* gene manifest as FOXG1 syndrome, a severe neurodevelopmental disorder characterized by structural brain anomalies, including agenesis of the corpus callosum, hippocampal reduction, and myelination delays. Despite the well-defined genetic basis of FOXG1 syndrome, therapeutic interventions targeting the underlying cause of the disorder are nonexistent. In this study, we explore the therapeutic potential of adeno-associated virus 9 (AAV9)-mediated delivery of the *FOXG1* gene. Remarkably, intracerebroventricular injection of AAV9-FOXG1 to *Foxg1* heterozygous mouse model at the postnatal stage rescues a wide range of brain pathologies. This includes the amelioration of corpus callosum deficiencies, the restoration of dentate gyrus morphology in the hippocampus, the normalization of oligodendrocyte lineage cell numbers, and the rectification of myelination anomalies. Our findings highlight the efficacy of AAV9-based gene therapy as a viable treatment strategy for FOXG1 syndrome and potentially other neurodevelopmental disorders with similar brain malformations, asserting its therapeutic relevance in postnatal stages.

INTRODUCTION

The recent advancement of genetic testing technology identified the genetic cause of many neurodevelopmental disorders and greatly facilitated the diagnosis of those disorders in clinics. A large proportion of genetically defined neurodevelopmental disorders is caused by the mutations of the genes that play an important role in brain development. Many such disorders are associated with brain structural deficits, such as microcephaly, corpus callosum agenesis, underdeveloped hippocampus, and myelination deficits. A pivotal but unresolved issue is if the perinatal brain malformations, particularly those originated by neuronal defects *in utero*, can be reversed by the treatment at postnatal stages by which the neurogenesis and axonal wiring are largely completed.

The FOXG1 syndrome (FS), also previously known as a congenital variant of Rett syndrome, results from mutations in a single allele of the *FOXG1* gene, and thus FS patients are heterozygous for *FOXG1* pathogenic variants.[1–3] Most FS is caused by *de novo* mutations in FS patients, although a small portion of FS is attributed to the gonadal mutations in parents of FS patients.[4] As FS is caused by the haploinsufficiency of *FOXG1* gene dosage, it is a suitable target for AAV9-directed gene therapy for normalizing FOXG1 levels. Notably, human magnetic resonance imaging studies revealed that FS is associated with severe brain structural deficits, including microcephaly, hypogenesis of the corpus callosum, delayed myelination, and hippocampus atrophy.[1–3,5] Clinically, FS is characterized by various symptoms, including profound intellectual disability, involuntary and continuous jerky movements, feeding problems, sleep disturbances, irritability, and excessive crying.[1–3,5] Additionally, many FS patients cannot speak or walk on their own and experience epilepsy. As FS patients display autistic features, including repetitive movements and poor social interaction skills, FS is considered an autism spectrum disorder (ASD).[3] Interestingly, the gene duplication for *FOXG1* is also linked to ASD.[6,7] In addition, the human *FOXG1* gene is one of the most strongly upregulated genes during neuronal differentiation of induced pluripotent stem cells (iPSCs) derived from a cohort of idiopathic ASD individuals.[8,9] FOXG1 has also been implicated in Alzheimer's disease, schizophrenia, and brain cancers.[3,10–13] These results highlight that controlling the FOXG1 dosage is crucial for human brain development and function.

The *FOXG1* gene encodes the transcription factor FOXG1, which is crucial for forebrain development.[14] In mice, complete elimination of the *Foxg1* gene results in a drastic reduction of the cerebral hemispheres in part due to reduced proliferation and precocious differentiation of FOXG1-deficient neural progenitors.[15,16] *Foxg1* haploinsufficiency in mice leads to disrupted forebrain development, resulting in neocortex reduction, hippocampus abnormalities, and corpus callosum agenesis,[14,17] like human FS.[1–3,5] This brain malformation upon the loss of one *Foxg1* allele is attributed to a decreased population of cortical intermediate progenitors and reduced supragranular cortical layers.[14,18,19] The axons of callosal neurons in the cerebral cortex extend across the midline of the brain and connect the two cortical hemispheres, forming the corpus callosum. Importantly, deletion of only one *Foxg1* allele in cortical neurons (*Foxg1*-conditional heterozygous mice, *Foxg1^{fl/+};NexCre,* herein referred to as *Foxg1*-cHet) recapitulated *Foxg1* haploinsufficiency conditions, including microcephaly, corpus callosum malformation, and reduction of the cortical upper layers,[14] suggesting that FOXG1 action in postmitotic neurons is required for the forebrain development.

Despite the recent advances in AAV9-directed gene therapy for central nervous system diseases,[20,21] the efficacy of this technology in correcting prenatal brain malformations associated with neurodevelopmental disorders remains unclear. To explore this critical issue, we assessed the effectiveness of postnatal administration of the *FOXG1* gene using the AAV9 vector to counteract brain structural deficits in a *Foxg1* haploinsufficiency mouse model. Our study reveals that postnatal injection of AAV9-FOXG1 substantially rescued the severe brain anatomical impairments observed in FS. Our results highlight that AAV9-directed gene therapy can be explored to treat neurodevelopmental disorders presenting with brain structural abnormality.

RESULTS

Foxg1-cHet mice show corpus callosum agenesis and anatomical changes in the hippocampus

The corpus callosum agenesis and microcephaly are the two cardinal features of human FS.[1–3] In mice, the generation of cortical projection neurons and their positioning within the cortex are accomplished by birth, resulting in the formation of a six-layered cerebral cortex. The callosal axonal bundles bridging the cortical hemispheres, which form the corpus callosum, are evident by embryonic day (E) 16.5, and the callosal connection is largely completed by postnatal day (P) 0 in mice.

Notably, *Foxg1*-cHet mice showed reduced cortex thickness and shortened corpus callosum,[14] similar to human FS brains.[1–3] The immunostaining with the axonal marker L1 (L1CAM) antibody revealed that the loss of corpus callosum was prominent in the posterior region of *Foxg1*-cHet brains at P3, compared with littermate control (*Foxg1^{fl/fl}* or *Foxg1^{fl/+}* without Cre) mice (Figure S1). These results suggest that the corpus callosum agenesis in *Foxg1* mutant mice is prenatal deficits driven by neuronal differentiation, neuronal migration, and axon guidance defects in embryonic brains.

To determine if *Foxg1*-cHet mice show hippocampal morphology changes similar to *Foxg1* global heterozygous mice,[17,22] we performed immunostaining analysis with antibody against CTIP2 (BCL11B), which is expressed in pyramidal cells in CA1 and CA2 areas and granular neurons in the dentate gyrus.[23] This analysis revealed prominent anatomical changes in the hippocampus of *Foxg1*-cHet brains at P27 (Figure 1A). Most strikingly, the length of the dentate gyrus was substantially reduced in *Foxg1*-cHet brains. The apex, where the enclosed blade and exposed blade meet, was wider in angle, and the overall "V" shape of the apex became unsharpened in the dentate gyrus of *Foxg1*-cHet mice. Overall, *Foxg1*-cHet mice showed marked morphological changes in the corpus callosum and hippocampus.

Foxg1-cHet mice display increased oligodendrocyte precursor cells

Although delayed myelination and reduced white matter volume were found frequently in FS,[1–3,5] the role of FOXG1 in developing oligodendrocytes remains unknown. Given that FOXG1 is expressed in oligodendrocyte precursor cells (OPCs) but downregulated as OPCs differentiate into oligodendrocytes (Figure S2),[24] we examined the number and distribution of OPCs in P27 *Foxg1*-cHet brains using immunostaining analysis with antibodies against OLIG2, a marker for the oligodendrocyte cell lineage with the highest expression in OPCs,[25,26] and myelin basic protein (MBP), a major myelin constituent and a marker for oligodendrocyte differentiation and myelination. Interestingly, the number of OLIG2$^+$ OPCs was markedly increased in the cortex of *Foxg1*-cHet mice (Figure 1B). In addition, the intensity of MBP$^+$ oligodendrocyte processes and branches were reduced, indicating a deficiency in myelination in *Foxg1*-cHet mice (Figure 1B). These data suggest a role of FOXG1 in oligodendrocyte development.

Generation and characterization of scAAV9-FOXG1 virus

To test if the delivery of the human *FOXG1* gene to *Foxg1*-cHet brains rescues any cellular and morphological phenotypes, we generated the self-complementary (sc) AAV9 vector, scAAV9-FOXG1, in which chicken beta-actin promoter (*pCBA*)[27] drives the expression of the codon-optimized human *FOXG1* gene (Figure 2A). To determine the transduction efficiency and cell types of human FOXG1 expression upon the delivery of scAAV9-FOXG1, we carried out an intracerebroventricular (ICV) injection of scAAV9-FOXG1 virus into wild-type mice at P1 and collected the brains at P15 and P22, and performed *RNAscope in situ* hybridization assay[28] with the fluorescence probe designed to detect only the exogenous human *FOXG1* mRNA but not the endogenous mouse *Foxg1* mRNA. As expected, human *FOXG1* mRNA was detected only in scAAV9-FOXG1 virus-injected brains, but not in uninjected control brains (Figure 2B), confirming that human *FOXG1 in situ* hybridization probe is specific to human *FOXG1* and does not detect mouse *Foxg1*. Our data indicate that scAAV9-FOXG1 drives the expression of human *FOXG1* mRNA in the brains. The distribution pattern of human *FOXG1* was similar between P15 and P22 (Figure 2B). Human *FOXG1* was expressed in the brain areas that express mouse *Foxg1* endogenously, such as the cerebral cortex, olfactory bulb, hippocampus, and striatum (Figures 2B
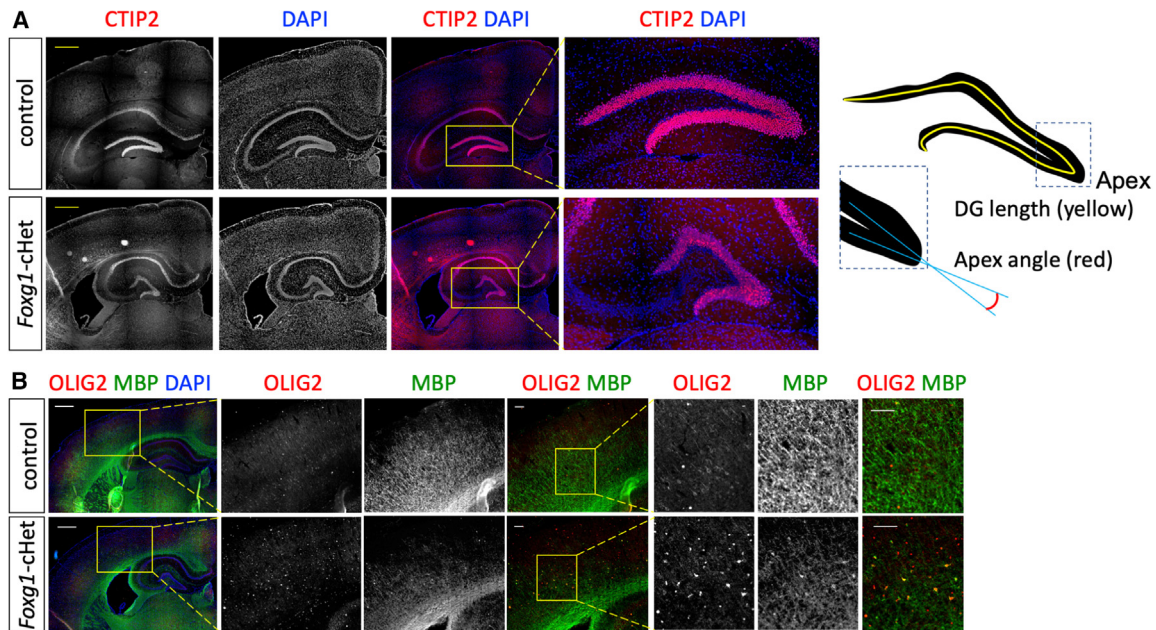
Figure 1. *Foxg1*-cHet brains display dentate gyrus abnormalities, aberrantly increased OLIG2⁺ oligodendrocyte lineage cells, and myelination deficiency

(A) Immunohistochemical analysis with CTIP2 antibody reveals prominent anatomical changes in the hippocampus of *Foxg1*-cHet brains at P27, including the shorter dentate gyrus length (yellow line in schematics) and wider apex angle between the two blades (red line in schematics). (B) Immunohistochemical analysis with antibodies against OLIG2 and MBP shows increased OLIG2⁺ OPCs and dysregulated MBP⁺ myelination patterns in P27 *Foxg1*-cHet brains. Scale bars, 500 µm (lower magnification images) or 100 µm (higher magnification images). *n* = 5 mice per condition. The representative images are shown.

and S3). In addition, it is also expressed in the brain regions lacking endogenous mouse *Foxg1* expression, such as the thalamus, cerebellum, pons, and medulla (Figure 2B).

Overall, the postnatal ICV injection of scAAV9-FOXG1 in mice triggered the expression of exogenous human *FOXG1* in mouse brains.

scAAV9-FOXG1 enhanced FOXG1 protein expression in *Foxg1*-cHet mice

The successful expression of human *FOXG1* following injection of scAAV9-FOXG1 in the postnatal brain prompted us to ask if scAAV9-FOXG1 can rescue phenotypes of *Foxg1*-cHet mice related to pathophysiology FS. To this end, we injected scAAV9-FOXG1 into *Foxg1*-cHet mice at P1 and analyzed their brains at P27.

We tested the expression of FOXG1 using *in situ* hybridization assays. Human *FOXG1*-specific *in situ* hybridization probe did not cross-react with mouse *Foxg1* mRNA, as shown by the absence of red fluorescence signal in control and *Foxg1*-cHet brains without scAAV9-FOXG1 (Figures 3A and S4). In scAAV9-FOXG1-injected *Foxg1*-cHet brains, human *FOXG1* mRNAs were expressed in mouse *Foxg1*-expressing regions, such as the cortex, hippocampus, striatum, and non-Foxg1-expressing areas, such as the thalamus (Figure 3A). Double *in situ* hybridization assays with human *FOXG1*-specific and mouse *Foxg1*-specific probes revealed that human *FOXG1* was expressed in mouse *Foxg1*-positive cells in the cortex, striatum, and

hippocampus, and was also detected in mouse *Foxg1*-negative cells in the thalamus (Figure S4).

To assess the distribution pattern and overall level of FOXG1 protein across different brain regions, we dissected specific brain areas and performed western blot (WB) analysis using FOXG1 antibody that recognizes both endogenous mouse FOXG1 and exogenous human FOXG1 (Figures 3B and S5). The mouse FOXG1 protein was detected in the cortex, hippocampus, striatum, and the sample combining thalamus and hypothalamus in control mice. *Foxg1*-cHet mice exhibited reduced FOXG1 levels in the cortex, hippocampus, and hypothalamus, where *Nex-Cre* is active,[29] but not in the striatum that does not express *Nex-Cre*. Interestingly, FOXG1 proteins were detected as double bands in scAAV9-FOXG1-injected brains, suggesting human FOXG1 protein-specific posttranslational modification. The overall FOXG1 protein levels were elevated in scAAV9-FOXG1-injected *Foxg1*-cHet brains relative to uninjected *Foxg1*-cHet brains.

To monitor changes in FOXG1 protein levels at the cellular scale, we conducted immunostaining analyses using two different FOXG1 antibodies and measured the fluorescence signal intensity in each FOXG1⁺ single cell in the cortex (Figures 3C–3E). FOXG1 protein levels were significantly reduced in *Foxg1*-cHet cortex relative to the control cortex. Consistent with *in situ* hybridization and WB results, administration of scAAV9-FOXG1 increased the overall FOXG1 protein levels in *Foxg1*-cHet cortex significantly
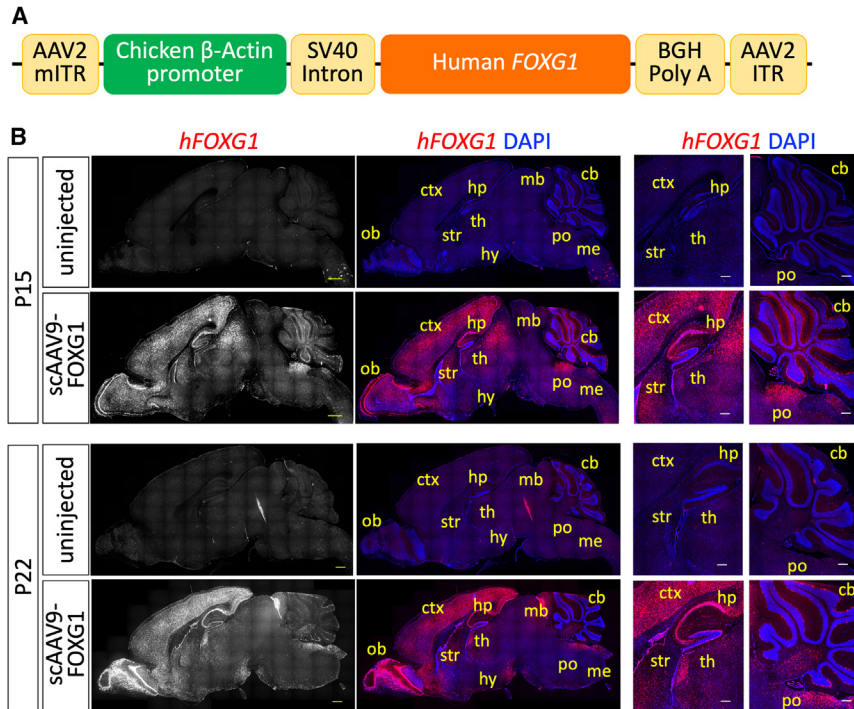
Figure 2. Expression of human *FOXG1* in mouse brains upon ICV injection of scAAV9-FOXG1

(A) Schematic representation of scAAV9-FOXG1 vector. (B) *In situ* hybridization analysis with the specific fluorescence probe against human *FOXG1* mRNA detects expression of human *FOXG1* in various regions of scAAV9-FOXG1-injected brains but not that of mouse *Foxg1* in uninjected control brains at P15 and P22. Scale bars, 5 mm (lower magnification images) or 2 mm (higher magnification images). ctx, cortex; ob, olfactory bulb; hp, hippocampus; str, striatum; th, thalamus; hy, hypothalamus; cb, cerebellum; po, pons; me, medulla; mb, midbrain. *n* = 3 mice per condition. The representative images are shown.

(Figures 3C–3E). Together, our data show that the reduced FOXG1 levels in *Foxg1*-cHet brains were restored upon injection of scAAV9-FOXG1.

scAAV9-FOXG1 restored the corpus callosum and cortical neurons in *Foxg1*-cHet mice

Next, we asked if the postnatal expression of FOXG1 can rescue the prenatal defects caused by *Foxg1* haploinsufficiency.[14,17,19] The abrupt disconnection of L1[+] callosal nerves at the midline and the formation of the Probst bundle were evident in the posterior cortex of *Foxg1*-cHet mice at P27 (Figures 4A and 4B), indicating that the corpus callosum agenesis is not reversed in *Foxg1*-cHet mice during postnatal brain maturation. Strikingly, the callosal connections were recovered in scAAV9-FOXG1-injected *Foxg1*-cHet brains (Figures 4A and 4B). The thickness of the corpus callosum in the anterior region was comparable between control and *Foxg1*-cHet brains and was not affected by scAAV9-FOXG1 injection (Figure S6).

To test if postnatal FOXG1 expression influences the number of cortical neurons, we assessed the number of CTIP2^{+} deep-layer neurons and upper-layer cells above the CTIP2^{+} layer. Intriguingly, scAAV9-FOXG1 injection rescued the reduced number of cortical neurons in *Foxg1*-cHet mice (Figures 4D and 4E), but it did not restore cortical thickness (Figure 4F).

Together, these data demonstrate that the postnatal expression of FOXG1 via scAAV9-FOXG1 was sufficient to rescue the corpus callosum agenesis and cortical neuronal reduction, the phenotypes established prenatally.

scAAV9-FOXG1 rescued dentate gyrus abnormalities in *Foxg1*-cHet mice

We tested if scAAV9-FOXG1 can reverse dentate gyrus abnormalities. Remarkably, neonatal injection of scAAV9-FOXG1 also rescued the shortened length of the dentate gyrus of *Foxg1*-cHet mice to a level comparable to the control dentate gyrus (Figures 5A and 5B). Further, the widened angle of the apex of the dentate gyrus was restored by scAAV9-FOXG1 (Figures 5A–5C). Our data indicate that the postnatal FOXG1 expression using scAAV9-FOXG1 rescues the hippocampal abnormalities.

scAAV9-FOXG1 normalized OPC numbers and restored myelination in *Foxg1*-cHet mice

Next, we examined if scAAV9-FOXG1 can affect the overproduction of OPCs and myelination defects in *Foxg1*-cHet brains. The quantification of OLIG2^{+} OPCs revealed that scAAV9-FOXG1 injection normalized the increased number of OPCs in *Foxg1*-cHet mice (Figures 6A and 6B). The immunostaining with MBP antibody revealed that scAAV9-FOXG1 injection restored the overall myelination pattern and MBP expression levels in the *Foxg1*-cHet cortex (Figures 6A–6C). Notably, the rescued callosal axons crossing the midline in the posterior *Foxg1*-cHet cortex were myelinated (Figure S7). Together, our data suggest that the postnatal injection of scAAV9-FOXG1 can resolve OPC and myelination deficits in the *Foxg1* haploinsufficiency condition.

DISCUSSION

In this paper, we showed that *Foxg1*-cHet mice exhibit deficits in the cortex, hippocampus, and myelination (Figure 7), recapitulating the primary brain phenotypes of FOXG1 haploinsufficiency, such as microcephaly, corpus callosum agenesis, underdeveloped hippocampus, and myelination defects.[1–3,5] Most FS patients are heavily dependent on caregivers throughout their lives due to severe neurological and behavioral issues. However, current medical treatments for FS prioritize only symptom management as there are no available options to remedy the underlying causes of the disease.
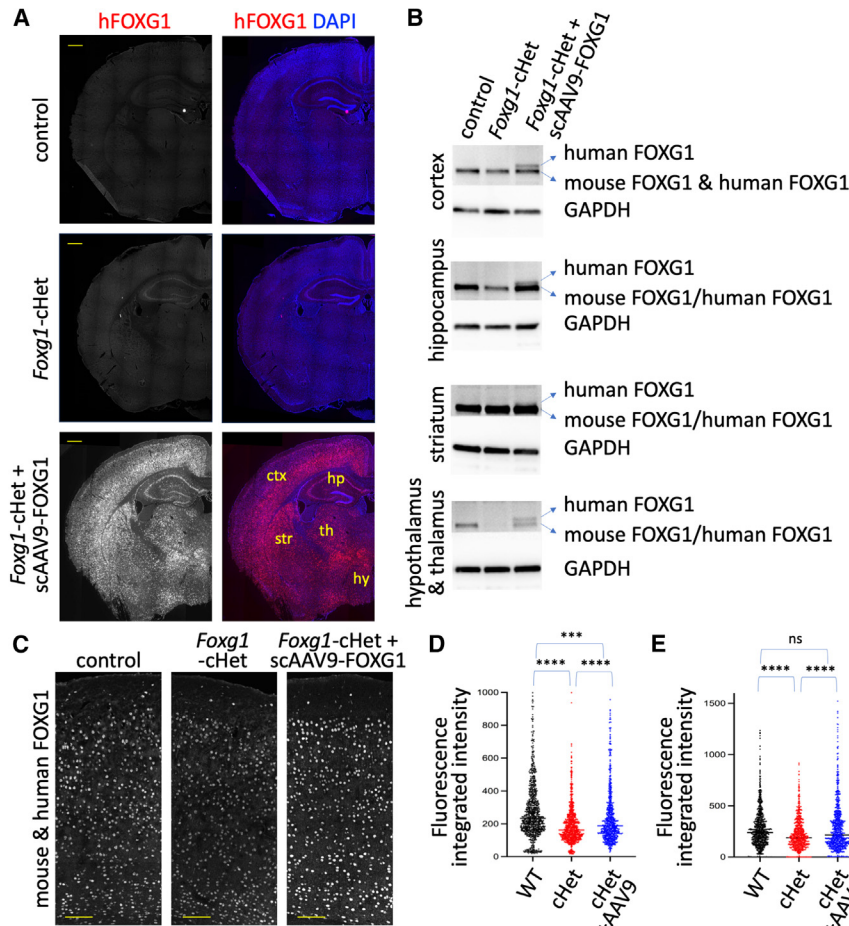
Figure 3. ICV injection of scAAV9-FOXG1 enhances FOXG1 levels in *Foxg1*-cHet brains

(A) *In situ* hybridization analysis with human *FOXG1* mRNA-specific fluorescence probe in P27 brains. Human *FOXG1* transcripts were detected in broad regions of scAAV9-FOXG1-injected *Foxg1*-cHet brain, but not in uninjected brains. Scale bars, 5 mm. ctx, cortex; hp, hippocampus; str, striatum; th, thalamus; hy, hypothalamus. (B–E) Western blotting (B) and immunostaining (C–E) analyses with FOXG1 antibodies, which recognize both endogenous mouse FOXG1 and exogenous human FOXG1, in P27 control, *Foxg1*-cHet, and scAAV9-FOXG1-injected *Foxg1*-cHet brains. (B) Reduced FOXG1 protein expression in *Foxg1*-cHet was restored by exogenous FOXG1 upon injection of scAAV9-FOXG1, as shown by WB in the cortex, hippocampus, and samples combining hypothalamus and thalamus (B) and immunostaining fluorescence intensity (C–E). (C) Scale bars, 100 μm. Two independent FOXG1 antibodies were used for fluorescence intensity quantification: Abcam ab196868 (D) and Sigma SAB2102981 (E). ***$p < 0.001$; ****$p < 0.0001$; ns, non-significant in one-way ANOVAs. $n = 700$–900 cells per condition.

neurons are primarily located in cortical layers II/III and V, and their production is completed by birth in mice.[32] The pronounced callosal axonal bundles are observed in newborn mice, but their myelination initiates after birth.[33] Notably, the mean diameter of unmyelinated axons remains constant during the active myelination phase in mice,[33] suggesting that the formation of callosal axonal bundles is primarily accomplished by birth. Agenesis of the corpus callosum is a brain abnormality that leads to a partial or total absence of the corpus callosum and is one of the most frequent congenital brain malformations, affecting three to seven people per 1,000 births.[34] The leading cause of corpus callosum agenesis is embryonic developmental abnormalities, such as dysregulated neuronal differentiation and axonal guidance.[34] Many neurodevelopmental disorders, including FS and autism, present with corpus callosum abnormalities.[1–3,5]

Given that the formation of the callosal axon bundle is accomplished prenatally, it is thought that corpus callosum agenesis is extremely difficult to resolve by postnatal treatment. Strikingly, our study revealed that postnatal expression of FOXG1 via scAAV9-FOXG1 injection can reconnect the callosal axons, leading to the substantial recovery of the corpus callosum. Notably, scAAV9-FOXG1 rescued the corpus callosum defects and the reduced cortical neuronal numbers. These results suggest that restoring the callosal nerves may involve axonal regrowth and the restoration of callosal neurons. Together, our results shed light on developing a gene therapy strategy for treating various neurodevelopmental conditions associated with prenatal brain abnormalities.
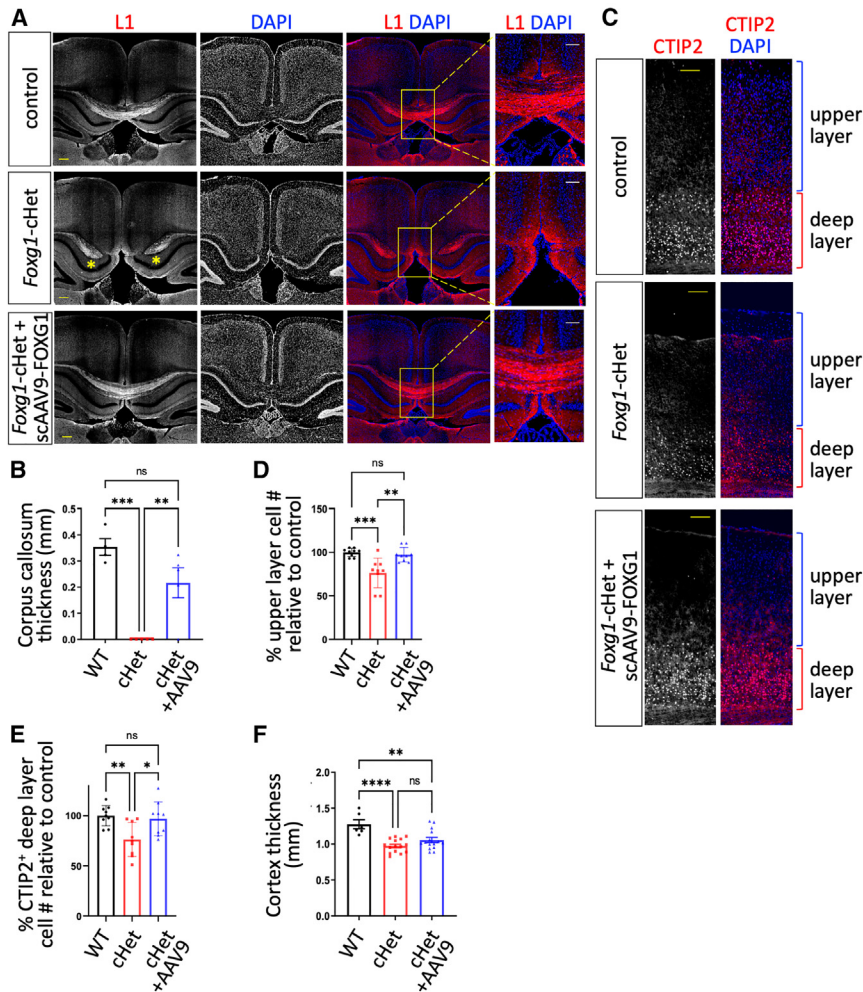
Therefore, there is an urgent unmet need to develop therapeutics for FS. Importantly, our studies uncovered that AAV9-directed delivery of FOXG1 after birth can rescue brain deficits of *FOXG1* haploinsufficiency, remarkably, including structural defects evident at birth (Figure 7). Thus, for the first time to our knowledge, our study proves the validity of the AAV9-directed gene therapy in treating FS and other neurodevelopmental disorders with similar brain structural defects.

Intriguingly, postnatal scAAV9-FOXG1 injection rescued the reduction of cortical neurons in the *Foxg1*-cHet cortex. Given that overall neurogenesis is completed by birth in mice and FOXG1 plays a role in promoting neuronal survival,[30] a plausible mechanism for neuronal rescue is that increased FOXG1 levels via scAAV9-FOXG1 injection prevented aberrant neuronal cell death in *Foxg1*-cHet cortex, rather than promoting the production of cortical neurons. This will be a significant topic for future studies.

The corpus callosum is a large bundle of myelinated axons that connect the two cerebral cortex hemispheres. Therefore, it facilitates the bilateral integration of sensory and motor information with social interactions, executive functions, and language.[31] Callosal projection

Figure 4. scAAV9-FOXG1 injection rescues the corpus callosum agenesis and reduces the number of cortical neurons in *Foxg1*-cHet brains

(A and B) Immunohistochemical analysis with the axonal marker L1 antibody in P27 brain sections containing the posterior corpus callosum. *Probost bundles. Scale bars, 200 μm (lower magnification images) or 100 μm (higher magnification images). (B) Quantification of posterior corpus callosum thickness. (C–F) Immunohistochemical analysis with the deep-layer marker CTIP2 antibody in P27 cortex. The upper-layer cells above CTIP2$^+$ cells (blue brackets, C) and CTIP2$^+$ deep-layer neurons (red brackets, C) were quantified in (D) and (E), respectively. (F) Quantification of the cortex thickness. The error bars represent the standard deviation of the mean. *$p < 0.05$; **$p < 0.01$; ***$p < 0.001$; ****$p < 0.0001$; ns, non-significant in one-way ANOVAs. $n = 5$ mice per condition. The representative images are shown.

The hippocampus is critical in memory, learning, and emotional behavior. The dentate gyrus is the primary gateway for input formation into the rest of the hippocampus and one of only a few brain areas of continuous adult neurogenesis in mammals.[35] The mammalian hippocampus formation starts early in embryos, but the hippocampus continues to develop in postnatal stages up to the first 4 weeks in mice.[35] Foxg1 plays an important role in both embryonic hippocampal morphogenesis and postnatal development of the dentate gyrus.[17,22,36] Accordingly, *Foxg1* heterozygous mice show markedly reduced hippocampus volume.[17,22] In particular, *Foxg1* global heterozygous mice exhibit a reduction of dentate granule cells due to impaired neurogenesis in the postnatal dentate gyrus, likely contributing to cognitive deficits in contextual fear conditioning.[4,37] Our study found that *Foxg1*-cHet mice also exhibited dentate gyrus abnormalities (Figures 5A and 7). Given the role of FOXG1 in both embryonic and postnatal hippocampus development, the remarkable rescue of dentate gyrus morphology by scAAV9-FOXG1 in *Foxg1*-cHet mice (Figures 5 and 7) is likely to be, at least partly, attributed to restoring postnatal FOXG1 action. These results suggest that the restoration of FOXG1 levels after birth may lead to the significant rescue of FS
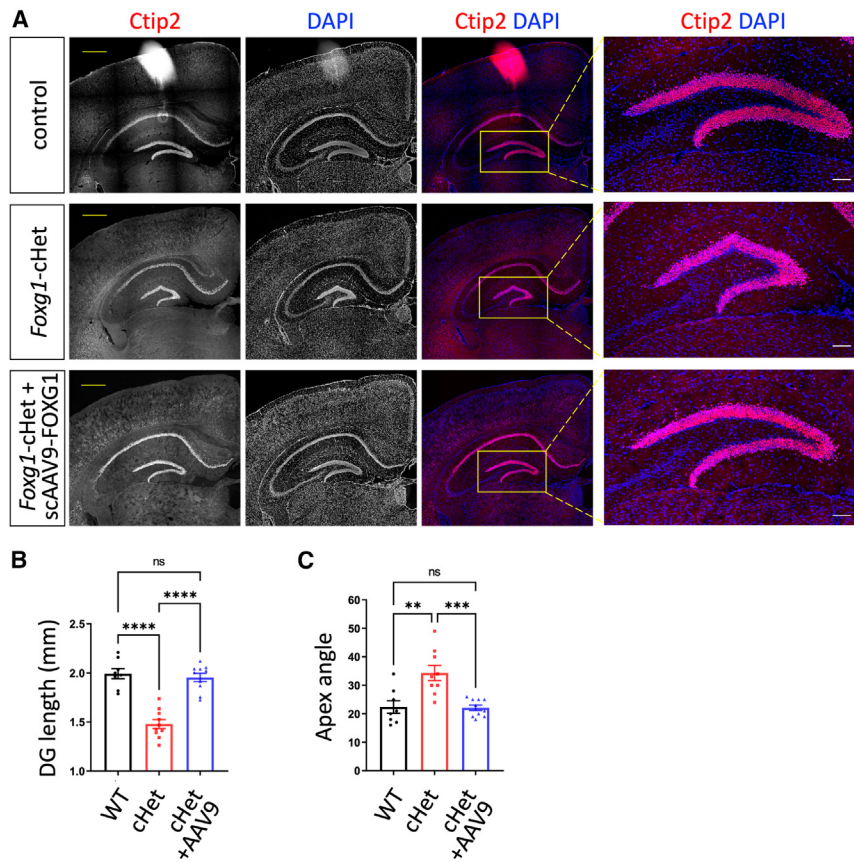
symptoms in humans as FOXG1 continues to play a crucial role in brain maturation and function.

Oligodendrocytes are primarily responsible for the myelination of axons in the brain to enable the rapid transmission of neural information. While delayed myelination is frequently observed in neuroimaging studies of FS patients,[1–3,5] the role of FOXG1 in oligodendrocyte lineage development remains elusive. Our studies uncovered that, in the developing brain, *Foxg1* haploinsufficiency results in increased OPCs and dysregulated myelination. This is consistent with the neuropathological finding that human fetal brains with *FOXG1* mutations display increased OPCs.[38] The molecular mechanism by which a reduced Foxg1 dosage leads to increased OPCs is an important subject for future studies with significant clinical implications. Given the expression of FOXG1 in OPCs, FOXG1 may play a key role in promoting OPC differentiation during brain development. It is also possible that OPCs increase to compensate for myelination deficits[39] caused by a lower level of FOXG1. In either case, *Foxg1* haploinsufficiency can increase OPCs and impair myelination. Intriguingly, our study uncovered that the postnatal injection of scAAV9-FOXG1 normalized the aberrantly increased OPCs and rectified myelination defects in *Foxg1*-cHet brains (Figures 6 and S7). These results suggest that FOXG1 gene therapy has potential therapeutic values in treating symptoms related to glial cells, such as delayed myelination.[1–3,5] The key question that warrants further investigation is if this exogenous FOXG1-mediated correction of myelination is due to the restored FOXG1 levels in glial or neuronal lineage. In this regard, it is noteworthy that a copy of the *Foxg1* gene is deleted by *Nex-Cre* in our *Foxg1*-cHet model.[14] Given that *Nex-Cre* is active in intermediated progenitor cells and cortical projection neurons,[29]

Figure 5. scAAV9-FOXG1 injection rescues the hippocampal malformation in *Foxg1*-cHet brains

(A) Immunohistochemical analysis with CTIP2 antibody reveals the restoration of the dentate gyrus length and apex angle in P27 *Foxg1*-cHet mice by neonatal injection of scAAV9-FOXG1. Scale bars, 500 μm (lower magnification images) or 100 μm (higher magnification images). (B and C) Quantification of dentate gyrus length (B) and apex angle (C). The error bars represent the standard deviation of the mean. $**p < 0.01$; $***p < 0.001$; $****p < 0.0001$; ns, non-significant in one-way ANOVAs. $n = 5$ mice per condition. The representative images are shown.

it is possible that a reduced FOXG1 level affected the fate of inter-mediated progenitor cells or other *Nex-Cre*-active progenitors to promote oligodendrocyte lineage status. Alternatively, reduced FOXG1 levels in neurons may affect oligodendrocyte homeostasis indirectly. Understanding the mechanisms of OPC normalization and myelination restoration will help design effective gene therapy for FS, as such gene therapy strategy may require the restoration of FOXG1 levels not only in neurons but also in neural progenitors and glial lineage.

In the future, the following points should be considered in devising more therapeutically relevant AAV9-FOXG1 vectors. First, given the crucial role of *FOXG1* gene dosage in human brain development and function[40] and the association of elevated FOXG1 expression with tumors,[12,41–43] it is important to achieve expression levels comparable to the endogenous FOXG1 levels. Second, since FOXG1 exhibits a cell-type-specific expression pattern in the brain rather than broadly expressed throughout the brain,[44] it will be ideal to restrict FOXG1 expression to endogenous FOXG1-expressing cell types. Third, as *Foxg1* heterozygous mouse models show FS-like behavioral deficits, such as hyperactivity, memory deficits, and social behavior deficits,[22,45] it can be evaluated if the therapeutic AAV9-FOXG1 rescues these behavioral phenotypes in addition to brain structural deficits in FS animal models. Fourth, it will be vital to determine the postnatal time window in which AAV9-FOXG1 can correct the brain structural and behavioral abnormalities in FS animal models.

In sum, we provide a proof-of-concept for AAV9-directed gene therapy in treating FS patients. We demonstrated that scAAV9-FOXG1 can successfully rescue several brain structural and cellular deficits related to human FS phenotypes,[1–3,5] including corpus callosum agenesis, dentate gyrus malformation, aberrant number of OPCs and neurons, and myelination defects, in the preclinical animal model of *Foxg1*-cHet mice (Figure 7). Our findings have substantial implications for clinical translation, particularly because scAAV9-FOXG1 was shown to have the potential to rescue the prenatally malformed brain structure.

MATERIALS AND METHODS

Viral preparation of scAAV9-FOXG1

A codon-optimized human FOXG1 coding sequence (CDS) construct was generated and commercially synthesized (Genscript, Piscataway, NJ). The human FOXG1 CDS was subcloned in AAV vectors under the chicken beta-actin promoter (pCBA), modified SV40 intron, and bovine growth hormone poly A terminator (Figure 2A). Self-complementary scAAV9-pCBA-FOXG1 was produced by transient transfection procedures using a double-stranded AAV2-ITR-based vector, with a plasmid encoding Rep2/Cap9 sequence as previously described,[46] along with an adenoviral helper plasmid pHelper (Stratagene, Santa Clara, CA) in HEK293 cells at Andelyn Biosciences (Columbus, OH).

Mice and ICV injection

The mice were housed at 12 h dark/12 h light cycle, 25°C, and 50% humidity conditions. All housing and analyses complied with the guidelines of the Institutional Animal Care and Use Committee of the University at Buffalo. *Foxg1^flox^* mouse[47] *and Nex-Cre*[29] lines were described previously. All experiments were conducted
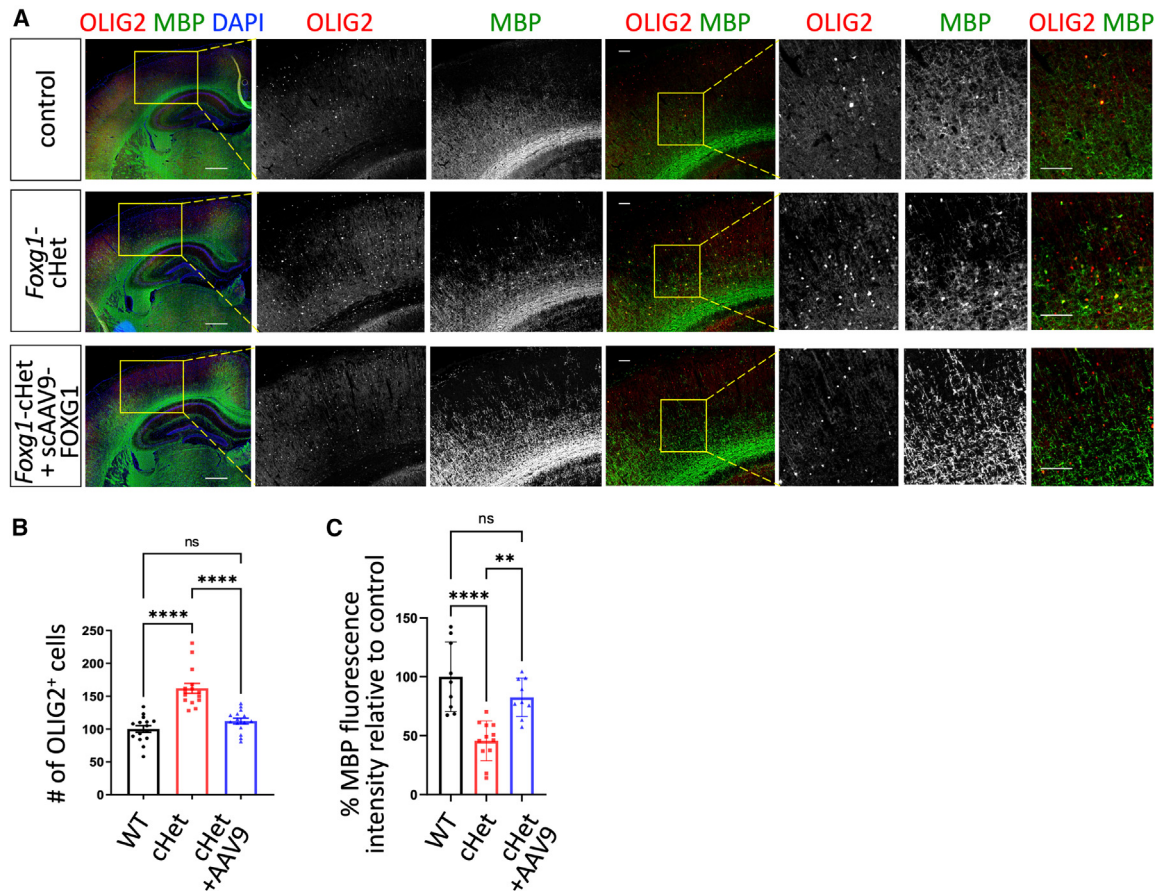
Figure 6. scAAV9-FOXG1 injection normalizes aberrantly increased OLIG2⁺ oligodendrocyte lineage cells and reduced myelination in *Foxg1*-cHet brains

(A) Immunohistochemical analysis with antibodies against OLIG2 and MBP reveals the normalized OLIG2⁺ cell numbers and the recovered myelination pattern in scAAV9-FOXG1-injected *Foxg1*-cHet brains compared with uninjected *Foxg1*-cHet brains. Scale bars, 500 μm (lower magnification images) or 100 μm (higher magnification images). (B and C) Quantification of OLIG2⁺ cells (B) and MBP fluorescence signals (C). The error bars represent the standard deviation of the mean. **p < 0.01; ****p < 0.0001; ns, non-significant in one-way ANOVAs. *n* = 5 mice per condition. The representative images are shown.

on mice with the C57BL/6 background, and *Foxg1-cHet* mice were generated by crossing *Foxg1ᶠˡᵒˣ/⁺* with *Nex-Cre* mice. Neonatal pups were ICV injected within 36 h after birth. ICV injection was performed under cryoanesthesia and using 10 μL Hamilton micro-syringe into the lateral ventricle of a single hemisphere. Each AAV9 virus was diluted to 1×10^{13} vg/mL and injected at a 5 μL volume per mouse.

RNA *in situ* hybridization

Expression of human *FOXG1* mRNA by AAV9 virus injected into mouse brains was analyzed by RNAscope (Advanced Cell Diagnostics) fluorescence *in situ* hybridization. The human *FOXG1*-specific probe was synthesized by Advanced Cell Diagnostics, and frozen brain sections of mice at indicated ages were cut in 20 μm. The brain sections were hybridized with human *FOXG1*-specific or mouse *Foxg1*-specific probe, and the signal was detected by incubating with Opal 570 fluorophore (Akoya Biosciences) according to the manufacturer's protocols. Three mouse brains and at least three sec-

tions of each brain were analyzed, and the representative images are shown in Figures 2B and 3A.

Immunohistochemical analysis and image acquisition

Dissected brains were fixed in 4% paraformaldehyde in phosphate-buffered saline at 4°C overnight, equilibrated in 30% sucrose, and embedded in Tissue Frozen Medium (Electron Microscopy Sciences) for frozen sectioning. Then, 18-μm brain sections were prepared on a cryostat (CM1950, Leica). Position-matched sections were stained using standard immunohistochemical techniques. Sections were stained with the primary antibody followed by secondary species-specific antibodies conjugated to fluorophores (Jackson ImmunoResearch), and then counterstained with DAPI to reveal nuclei. The primary antibodies include rabbit anti-OLIG2 (Millipore AB15328, 1:1000), rat anti-L1 (NCAM) (Millipore MAB5272, 1:1000), rat anti-CTIP2 (Abcam AB18465, 1:1000), rat anti-MBP (Millipore MAB386, 1:500), rabbit anti-FOXG1 (Sigma SAB2102981, 1:1000) and rabbit anti-FOXG1 (Abcam ab196868, 1:1000) antibodies. The secondary

Structural & cellular defects rescued by scAAV9-FOXG1
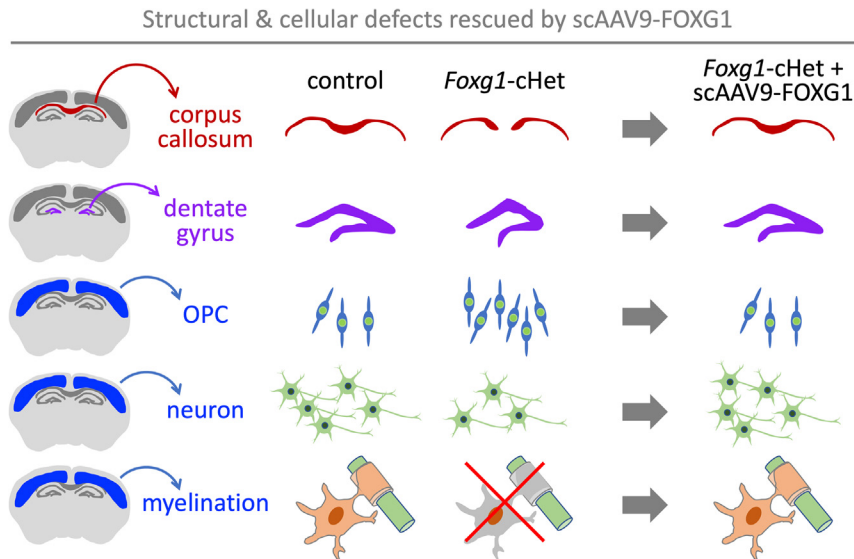
antibodies from Jackson ImmunoResearch Laboratories include donkey anti-rat Cy3 (Cat.712-165-153, 1:500), donkey anti-rabbit Alexa Fluor 647 (Cat.711-605-152, 1:500), and goat anti-rat Alexa Fluor 594 (Cat.112-585-167, 1:500).

Image data were collected through a DM6 fluorescence microscope and analyzed by Leica Software LasX. Images were further processed using Photoshop CS5 (Adobe, San Jose, CA). Counting on OLIG2 positive cells was conducted using five brain sections per mouse. In each brain section, three areas were selected to count in the cortex. One region of interest (ROI) (x = 1 mm; y = cortex thickness) per each area immunostained with anti-OLIG2 was counted for the number of positive cells.

High-resolution confocal images (60× magnification, 2 × 4 tiles) were employed in CellProfiler[48] for the automated quantification of immunofluorescent intensity in each cortex cell. The following pipeline was implemented: The Crop module was utilized to eliminate unnecessary areas in the images. The Identify Primary Objects module, employing Global thresholding, the Otsu approach, and based on object intensity settings, was employed to recognize FOXG1 antibody immunostaining signal in each individual cell. The settings were adjusted to capture all positive signaling while minimizing noise. The Measure Object Intensity module was used to generate intensity data for further analysis. The Export to Spreadsheet module was applied to export all data into Excel format for subsequent processing. The integrated intensity represents the sum of pixel intensities over all pixels in a cell.

WB analysis

The cortex, hippocampus, striatum, and hypothalamus and thalamus tissues were lysed in RIPA buffer (Cell Signaling, #9806) supplemented with Protease Inhibitor Cocktail (Cell Signaling, #5870) for 1 h at 4°C. Protein concentrations were determined using a BCA protein assay kit (Thermo, 23225). Subsequently, 10 μg of protein per well was loaded onto Novex Tris-Glycine Mini Protein Gels, 10%–20% (Thermo, XP10202BOX), and electrophoresis was conducted at 100 V for 1.5 h. Proteins were then transferred to a 0.22-μm PVDF membrane using the eBlot transfer kit (GenScript). Following blocking in 5% nonfat milk for 1 h, the membrane was cut into bands and incubated overnight at 4°C with FOXG1 (1:1000, Abcam, ab196868) and GAPDH (1:1,000, Thermo, MA1-16757) antibodies. Next, the membrane was rinsed five times in TBST, and then incubated with the corresponding secondary antibodies at room temperature for 1 h, rinsed five times with TBST, and developed with Pierce ECL Western Blotting Substrate (Thermo, 32109).

Statistical analyses

The data were analyzed using GraphPad 9 (Prism, San Diego, CA). One-way ANOVAs were run using genotype as between-subject variables. A repeated-measures ANOVA was used to analyze values of OLIG2-positive cell counting and DG length measuring. All bars and error bars represent the mean ± SEM, and significance was set at $p < 0.05$ (****$p < 0.0001$; ***$p < 0.001$; **$p < 0.01$; *$p < 0.05$; ns, not significant).

DATA AND CODE AVAILABILITY

The authors confirm that the data supporting the findings of this study are available within the article and its supplemental information, and that there are no data deposited in any repository.

SUPPLEMENTAL INFORMATION

Supplemental information can be found online at https://doi.org/10.1016/j.omtm.2024.101275.

ACKNOWLEDGMENTS

AUTHOR CONTRIBUTIONS

DECLARATION OF INTERESTS

REFERENCES

1. Srivastava, S., Desai, S., Cohen, J., Smith-Hicks, C., Barañano, K., Fatemi, A., and Naidu, S. (2018). Monogenic disorders that mimic the phenotype of Rett syndrome. Neurogenetics 19, 41–47. https://doi.org/10.1007/s10048-017-0535-3.

2. Ehrhart, F., Sangani, N.B., and Curfs, L.M.G. (2018). Current developments in the genetics of Rett and Rett-like syndrome. Curr. Opin. Psychiatry 31, 103–108. https://doi.org/10.1097/yco.0000000000000389.

3. Vegas, N., Cavallin, M., Maillard, C., Boddaert, N., Toulouse, J., Schaefer, E., Lerman-Sagie, T., Lev, D., Magalie, B., Moutton, S., et al. (2018). Delineating FOXG1 syndrome: From congenital microcephaly to hyperkinetic encephalopathy. Neurol. Genet. 4, e281. https://doi.org/10.1212/nxg.0000000000000281.

4. McMahon, K.Q., Papandreou, A., Ma, M., Barry, B.J., Mirzaa, G.M., Dobyns, W.B., Scott, R.H., Trump, N., Kurian, M.A., and Paciorkowski, A.R. (2015). Familial recurrences of FOXG1-related disorder: Evidence for mosaicism. Am. J. Med. Genet. 167a, 3096–3102. https://doi.org/10.1002/ajmg.a.37353.

5. Harada, K., Yamamoto, M., Konishi, Y., Koyano, K., Takahashi, S., Namba, M., and Kusaka, T. (2018). Hypoplastic hippocampus in atypical Rett syndrome with a novel FOXG1 mutation. Brain Dev. 40, 49–52. https://doi.org/10.1016/j.braindev.2017.07.007.

6. Brunetti-Pierri, N., Paciorkowski, A.R., Ciccone, R., Della Mina, E., Bonaglia, M.C., Borgatti, R., Schaaf, C.P., Sutton, V.R., Xia, Z., Jelluma, N., et al. (2011). Duplications of FOXG1 in 14q12 are associated with developmental epilepsy, mental retardation, and severe speech impairment. Eur. J. Hum. Genet. 19, 102–107. https://doi.org/10.1038/ejhg.2010.142.

7. Yeung, A., Bruno, D., Scheffer, I.E., Carranza, D., Burgess, T., Slater, H.R., and Amor, D.J. (2009). 4.45 Mb microduplication in chromosome band 14q12 including FOXG1 in a girl with refractory epilepsy and intellectual impairment. Eur. J. Med. Genet. 52, 440–442. https://doi.org/10.1016/j.ejmg.2009.09.004.

8. Marchetto, M.C., Belinson, H., Tian, Y., Freitas, B.C., Fu, C., Vadodaria, K., Beltrao-Braga, P., Trujillo, C.A., Mendes, A.P.D., Padmanabhan, K., et al. (2017). Altered proliferation and networks in neural cells derived from idiopathic autistic individuals. Mol. Psychiatry 22, 820–835. https://doi.org/10.1038/mp.2016.95.

9. Mariani, J., Coppola, G., Zhang, P., Abyzov, A., Provini, L., Tomasini, L., Amenduni, M., Szekely, A., Palejev, D., Wilson, M., et al. (2015). FOXG1-Dependent Dysregulation of GABA/Glutamate Neuron Differentiation in Autism Spectrum Disorders. Cell 162, 375–390. https://doi.org/10.1016/j.cell.2015.06.034.

10. Won, H., de la Torre-Ubieta, L., Stein, J.L., Parikshak, N.N., Huang, J., Opland, C.K., Gandal, M.J., Sutton, G.J., Hormozdiari, F., Lu, D., et al. (2016). Chromosome conformation elucidates regulatory relationships in developing human brain. Nature 538, 523–527. https://doi.org/10.1038/nature19847.

11. Ma, Y., Jun, G.R., Zhang, X., Chung, J., Naj, A.C., Chen, Y., Bellenguez, C., Hamilton-Nelson, K., Martin, E.R., Kunkle, B.W., et al. (2019). Analysis of Whole-Exome Sequencing Data for Alzheimer Disease Stratified by APOE Genotype. JAMA Neurol. 76, 1099–1108. https://doi.org/10.1001/jamaneurol.2019.1456.

12. Adesina, A.M., Nguyen, Y., Mehta, V., Takei, H., Stangeby, P., Crabtree, S., Chintagumpala, M., and Gumerlock, M.K. (2007). FOXG1 dysregulation is a frequent event in medulloblastoma. J. Neuro Oncol. 85, 111–122. https://doi.org/10.1007/s11060-007-9394-3.

13. Verginelli, F., Perin, A., Dali, R., Fung, K.H., Lo, R., Longatti, P., Guiot, M.C., Del Maestro, R.F., Rossi, S., di Porzio, U., et al. (2013). Transcription factors FOXG1 and Groucho/TLE promote glioblastoma growth. Nat. Commun. 4, 2956. https://doi.org/10.1038/ncomms3956.

14. Cargnin, F., Kwon, J.S., Katzman, S., Chen, B., Lee, J.W., and Lee, S.K. (2018). FOXG1 Orchestrates Neocortical Organization and Cortico-Cortical Connections. Neuron 100, 1083–1096.e5. https://doi.org/10.1016/j.neuron.2018.10.016.

15. Hanashima, C., Li, S.C., Shen, L., Lai, E., and Fishell, G. (2004). Foxg1 suppresses early cortical cell fate. Science 303, 56–59. https://doi.org/10.1126/science.1090674.

16. Xuan, S., Baptista, C.A., Balas, G., Tao, W., Soares, V.C., and Lai, E. (1995). Winged helix transcription factor BF-1 is essential for the development of the cerebral hemispheres. Neuron 14, 1141–1152.

17. Eagleson, K.L., Schlueter McFadyen-Ketchum, L.J., Ahrens, E.T., Mills, P.H., Does, M.D., Nickols, J., and Levitt, P. (2007). Disruption of Foxg1 expression by knock-in of cre recombinase: effects on the development of the mouse telencephalon. Neuroscience 148, 385–399. https://doi.org/10.1016/j.neuroscience.2007.06.012.

18. Siegenthaler, J.A., Tremper-Wells, B.A., and Miller, M.W. (2008). Foxg1 haploinsufficiency reduces the population of cortical intermediate progenitor cells: effect of increased p21 expression. Cereb. Cortex 18, 1865–1875. https://doi.org/10.1093/cercor/bhm209.

19. Pringsheim, M., Mitter, D., Schröder, S., Warthemann, R., Plümacher, K., Kluger, G., Baethmann, M., Bast, T., Braun, S., Büttel, H.M., et al. (2019). Structural brain anomalies in patients with FOXG1 syndrome and in Foxg1+/- mice. Ann. Clin. Transl. Neurol. 6, 655–668. https://doi.org/10.1002/acn3.735.

20. Ravi, B., Chan-Cortés, M.H., and Sumner, C.J. (2021). Gene-Targeting Therapeutics for Neurological Disease: Lessons Learned from Spinal Muscular Atrophy. Annu. Rev. Med. 72, 1–14. https://doi.org/10.1146/annurev-med-070119-115459.

21. Lykken, E.A., Shyng, C., Edwards, R.J., Rozenberg, A., and Gray, S.J. (2018). Recent progress and considerations for AAV gene therapies targeting the central nervous system. J. Neurodev. Disord. 10, 16. https://doi.org/10.1186/s11689-018-9234-0.

22. Shen, L., Nam, H.S., Song, P., Moore, H., and Anderson, S.A. (2006). FoxG1 haploinsufficiency results in impaired neurogenesis in the postnatal hippocampus and contextual memory deficits. Hippocampus 16, 875–890. https://doi.org/10.1002/hipo.20218.

23. Leid, M., Ishmael, J.E., Avram, D., Shepherd, D., Fraulob, V., and Dollé, P. (2004). CTIP1 and CTIP2 are differentially expressed during mouse embryogenesis. Gene Expr. Patterns 4, 733–739. https://doi.org/10.1016/j.modgep.2004.03.009.

24. Marques, S., Zeisel, A., Codeluppi, S., van Bruggen, D., Mendanha Falcão, A., Xiao, L., Li, H., Häring, M., Hochgerner, H., Romanov, R.A., et al. (2016). Oligodendrocyte heterogeneity in the mouse juvenile and adult central nervous system. Science 352, 1326–1329. https://doi.org/10.1126/science.aaf6463.

25. Lu, Q.R., Yuk, D., Alberta, J.A., Zhu, Z., Pawlitzky, I., Chan, J., McMahon, A.P., Stiles, C.D., and Rowitch, D.H. (2000). Sonic hedgehog–regulated oligodendrocyte lineage genes encoding bHLH proteins in the mammalian central nervous system. Neuron 25, 317–329. https://doi.org/10.1016/s0896-6273(00)80897-1.

26. Zhou, Q., Wang, S., and Anderson, D.J. (2000). Identification of a novel family of oligodendrocyte lineage-specific basic helix-loop-helix transcription factors. Neuron 25, 331–343. https://doi.org/10.1016/s0896-6273(00)80898-3.

27. Klein, R.L., Dayton, R.D., Tatom, J.B., Henderson, K.M., and Henning, P.P. (2008). AAV8, 9, Rh10, Rh43 vector gene transfer in the rat brain: effects of serotype, promoter and purification method. Mol. Ther. 16, 89–96. https://doi.org/10.1038/sj.mt.6300331.

28. Wang, F., Flanagan, J., Su, N., Wang, L.C., Bui, S., Nielson, A., Wu, X., Vo, H.T., Ma, X.J., and Luo, Y. (2012). RNAscope: a novel in situ RNA analysis platform for formalin-fixed, paraffin-embedded tissues. J. Mol. Diagn. 14, 22–29. https://doi.org/10.1016/j.jmoldx.2011.08.002.

29. Goebbels, S., Bormuth, I., Bode, U., Hermanson, O., Schwab, M.H., and Nave, K.A. (2006). Genetic targeting of principal neurons in neocortex and hippocampus of NEX-Cre mice. Genesis 44, 611–621. https://doi.org/10.1002/dvg.20256.

30. Dastidar, S.G., Landrieu, P.M.Z., and D'Mello, S.R. (2011). FoxG1 promotes the survival of postmitotic neurons. J. Neurosci. 31, 402–413. https://doi.org/10.1523/jneurosci.2897-10.2011.

31. Paul, L.K., Van Lancker-Sidtis, D., Schieffer, B., Dietrich, R., and Brown, W.S. (2003). Communicative deficits in agenesis of the corpus callosum: nonliteral language and affective prosody. Brain Lang. 85, 313–324. https://doi.org/10.1016/s0093-934x(03)00062-2.

32. Wise, S.P. (1975). The laminar organization of certain afferent and efferent fiber systems in the rat somatosensory cortex. Brain Res. *90*, 139–142. https://doi.org/10.1016/0006-8993(75)90688-5.

33. Sturrock, R.R. (1980). Myelination of the mouse corpus callosum. Neuropathol. Appl. Neurobiol. *6*, 415–420. https://doi.org/10.1111/j.1365-2990.1980.tb00219.x.

34. Fitsiori, A., Nguyen, D., Karentzos, A., Delavelle, J., and Vargas, M.I. (2011). The corpus callosum: white matter or terra incognita. Br. J. Radiol. *84*, 5–18. https://doi.org/10.1259/bjr/21946513.

35. Muramatsu, R., Ikegaya, Y., Matsuki, N., and Koyama, R. (2007). Neonatally born granule cells numerically dominate adult mice dentate gyrus. Neuroscience *148*, 593–598. https://doi.org/10.1016/j.neuroscience.2007.06.040.

36. Tian, C., Gong, Y., Yang, Y., Shen, W., Wang, K., Liu, J., Xu, B., Zhao, J., and Zhao, C. (2012). Foxg1 has an essential role in postnatal development of the dentate gyrus. J. Neurosci. *32*, 2931–2949. https://doi.org/10.1523/jneurosci.5240-11.2012.

37. Younger, S., Boutros, S., Cargnin, F., Jeon, S., Lee, J.W., Lee, S.K., and Raber, J. (2022). Behavioral Phenotypes of Foxg1 Heterozygous Mice. Front. Pharmacol. *13*, 927296. https://doi.org/10.3389/fphar.2022.927296.

38. Wilpert, N.M., Marguet, F., Maillard, C., Guimiot, F., Martinovic, J., Drunat, S., Attié-Bitach, T., Razavi, F., Tessier, A., Capri, Y., et al. (2021). Human neuropathology confirms projection neuron and interneuron defects and delayed oligodendrocyte production and maturation in FOXG1 syndrome. Eur. J. Med. Genet. *64*, 104282. https://doi.org/10.1016/j.ejmg.2021.104282.

39. Hughes, E.G., Kang, S.H., Fukaya, M., and Bergles, D.E. (2013). Oligodendrocyte progenitors balance growth with self-repulsion to achieve homeostasis in the adult brain. Nat. Neurosci. *16*, 668–676. https://doi.org/10.1038/nn.3390.

40. Hettige, N.C., and Ernst, C. (2019). FOXG1 Dose in Brain Development. Front. Pediatr. *7*, 482. https://doi.org/10.3389/fped.2019.00482.

41. Adesina, A.M., Nguyen, Y., Guanaratne, P., Pulliam, J., Lopez-Terrada, D., Margolin, J., and Finegold, M. (2007). FOXG1 is overexpressed in hepatoblastoma. Hum. Pathol. *38*, 400–409. https://doi.org/10.1016/j.humpath.2006.09.003.

42. Chan, D.W., Liu, V.W.S., To, R.M.Y., Chiu, P.M., Lee, W.Y.W., Yao, K.M., Cheung, A.N.Y., and Ngan, H.Y.S. (2009). Overexpression of FOXG1 contributes to TGF-beta resistance through inhibition of p21WAF1/CIP1 expression in ovarian cancer. Br. J. Cancer *101*, 1433–1443. https://doi.org/10.1038/sj.bjc.6605316.

43. Chen, J., Wu, X., Xing, Z., Ma, C., Xiong, W., Zhu, X., and He, X. (2018). FOXG1 Expression Is Elevated in Glioma and Inhibits Glioma Cell Apoptosis. J. Cancer *9*, 778–783. https://doi.org/10.7150/jca.22282.

44. Tao, W., and Lai, E. (1992). Telencephalon-restricted expression of BF-1, a new member of the HNF-3/fork head gene family, in the developing rat brain. Neuron *8*, 957–966. https://doi.org/10.1016/0896-6273(92)90210-5.

45. Miyoshi, G., Ueta, Y., Natsubori, A., Hiraga, K., Osaki, H., Yagasaki, Y., Kishi, Y., Yanagawa, Y., Fishell, G., Machold, R.P., and Miyata, M. (2021). FoxG1 regulates the formation of cortical GABAergic circuit during an early postnatal critical period resulting in autism spectrum disorder-like phenotypes. Nat. Commun. *12*, 3773. https://doi.org/10.1038/s41467-021-23987-z.

46. Foust, K.D., Nurre, E., Montgomery, C.L., Hernandez, A., Chan, C.M., and Kaspar, B.K. (2009). Intravascular AAV9 preferentially targets neonatal neurons and adult astrocytes. Nat. Biotechnol. *27*, 59–65. https://doi.org/10.1038/nbt.1515.

47. Miyoshi, G., and Fishell, G. (2012). Dynamic FoxG1 expression coordinates the integration of multipolar pyramidal neuron precursors into the cortical plate. Neuron *74*, 1045–1058. https://doi.org/10.1016/j.neuron.2012.04.025.

48. Stirling, D.R., Swain-Bowden, M.J., Lucas, A.M., Carpenter, A.E., Cimini, B.A., and Goodman, A. (2021). CellProfiler 4: improvements in speed, utility and usability. BMC Bioinf. *22*, 433. https://doi.org/10.1186/s12859-021-04344-9.